Available online at www.sciencedirect.com

ScienceDirect

Mendeleev Commun., 2017, **27**, 515–517

Mendeleev Communications

Single-atom Pd sites on the surface of Pd–In nanoparticles supported on γ-Al_2O_3: a CO-DRIFTS study

Aleksandr Yu. Stakheev,*[a] Nadezhda S. Smirnova,[a] Dmitry S. Krivoruchenko,[a] Galina N. Baeva,[a] Igor S. Mashkovsky,[a] Ilya A. Yakushev[b] and Michael N. Vargaftik[b]

[a] *N. D. Zelinsky Institute of Organic Chemistry, Russian Academy of Sciences, 119991 Moscow, Russian Federation. Fax: +7 499 135 5328; e-mail: st@ioc.ac.ru*

[b] *N. S. Kurnakov Institute of General and Inorganic Chemistry, Russian Academy of Sciences, 119991 Moscow, Russian Federation*

DOI: 10.1016/j.mencom.2017.09.029

The CO-DRIFTS investigation of a Pd–In catalyst obtained *via* the $PdIn(AcO)_5$ complex showed the presence of single palladium atoms isolated by indium on the surface. A short-time exposure to air under ambient conditions induced the decomposition of the single-atom structure, which can be recovered by mild reduction.

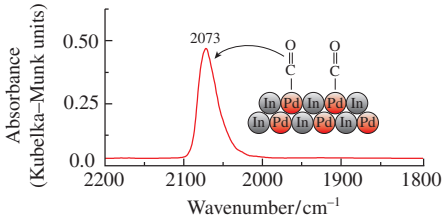

The acceleration of modern industrial production leads to the development of catalytic systems for complex transformations of organic molecules with ultrahigh selectivity.[1] Due to its high activity, palladium is widely applied as an active component of commercial supported catalysts in numerous chemical processes, including selective alkyne hydrogenation. The insufficient selectivity of palladium can be improved by the introduction of a second metal (Cu, Fe, Ag, Zn, Ga, In, *etc.*) resulting in the formation of a bimetallic phase.[2–4] Recently, special attention has been paid to the design of bimetallic systems with well-ordered structures, where the surface palladium atoms are isolated by other metal atoms (single-atom structures).[5–7] The main advantage of the catalysts with the single-atom structure in selective alkyne hydrogenation is their high selectivity for alkene production.[8] However, many alloys tend to undergo segregation and/or phase separation under reaction conditions, which deteriorates their catalytic characteristics.[9] This obstacle can be overcame by obtaining the single-atom structure on the surface of intermetallic compounds that leads to a superior structural stability, as compared to that of disordered substitutional alloys. For example, the Pd–Ga catalysts retained the isolation of Pd active sites during gas-phase acetylene hydrogenation providing enhanced stability and selectivity.[10]

Another promising system is the Pd–In catalyst capable of forming stable intermetallic species. The stable Pd–In intermetallic bulk structure with a well-defined composition can be obtained during the reduction of Pd/In_2O_3.[11] As in the case of a Pd–Ga intermetallic compound, the characteristic feature of the Pd–In intermetallic phase is the formation of isolated palladium sites.[12] This is in agreement with the results of our previous studies, which revealed improved selectivity for Pd–In in the selective hydrogenation of terminal and internal alkynes in a liquid phase.[3,13]

In spite of the increased attention to Pd–In catalysts, their surface characteristics are explored insufficiently. Therefore, this work was focused on studying the surface structure of a $Pd–In/Al_2O_3$ catalyst by the diffuse reflectance infrared Fourier transform spectroscopy of chemisorbed CO (CO DRIFTS).[†] Particular attention was paid to revealing the structure of Pd active sites and their stability to oxidation.

Figure 1 shows the DRIFT spectra of bimetallic $Pd–In/Al_2O_3$ and monometallic Pd/Al_2O_3 in the carbonyl region (1800–2200 cm^{-1}). The spectrum of the reference monometallic Pd/Al_2O_3 exhibits two bands: a narrower one in the region of 2120–2020 cm^{-1} centered at 2090 cm^{-1} and a broad band in the region of 2000–1800 cm^{-1} with a maximum at 1978 cm^{-1}. These bands were assigned to CO linearly adsorbed on metallic Pd (2090 cm^{-1}) and to multibonded CO (1978 cm^{-1}) combining bridged (2000–1895 cm^{-1}) and threefold bridged CO species (1920–1830 cm^{-1}).[15–17]

In contrast to the spectrum of monometallic Pd/Al_2O_3, the bimetallic $Pd–In/Al_2O_3$ sample exhibits an intense single band centered at 2073 cm^{-1} attributable to CO linearly adsorbed on metallic Pd. The absence of any distinguishable signal within the range of multibonded CO (2000–1800 cm^{-1}) provides strong

[†] The 1% Pd–1.08% In/Al_2O_3 (wt%, the molar ratio Pd : In = 1 : 1) catalyst was obtained *via* the $PdIn(AcO)_5$ heterometallic acetate complex as a precursor of the active component in accordance with a procedure described elsewhere.[14] The sample was reduced at 500 °C in a 5% H_2/Ar flow for 2 h. The previous TEM characterization of the catalyst indicated the presence of metallic nanoparticles of size 4–5 nm.[14] The reference sample was monometallic 1.0 wt% Pd/Al_2O_3. The catalyst was prepared by incipient wetness impregnation with an aqueous solution of $[Pd(NH_3)_4]Cl_2 \cdot H_2O$ with the subsequent calcination at 550 °C in an air flow for 4 h and reduction at 500 °C in a 5% H_2/Ar flow for 1 h. According to the TEM data, the particle size of palladium clusters was 3.5–4.0 nm.

The DRIFTS measurements were performed on a Tensor 27 Bruker spectrometer. The sample compartment of a cell (collector from Harrick) was filled with the as prepared sample. The sample (~20 mg) was first reduced *in situ* in a flow of 5 vol% H_2/Ar at 350 °C for 2 h. Then, the cell was cooled to 25 °C (oxidative experiments) or 50 °C (other experiments) and purged with Ar. A background spectrum was recorded under Ar. Then, a flow (30 cm^3 min^{-1}) of 0.5 vol% CO in He was introduced, and spectra were recorded at 50 °C; or the cell was purged with 20 vol% O_2/N_2 at 25 °C, and then a flow (30 cm^3 min^{-1}) of 0.5 vol% CO in He was introduced and spectra were recorded.

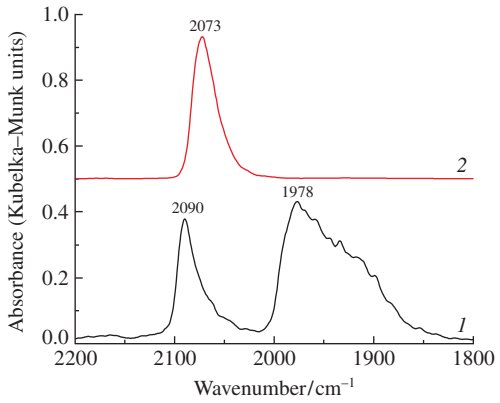

Figure 1 FTIR-CO spectra for (*1*) Pd/Al_2O_3 and (*2*) $Pd–In/Al_2O_3$.

evidence that the surface of Pd–In nanoparticles possesses solely single Pd atoms capable of binding CO only in a linear form without any ensembles of neighboring Pd atoms. The destabilization of bridging and hollow sites is presumably induced by increasing Pd–Pd interatomic distances due to Pd site isolation by In atoms similarly to the Pd–Ga system.[18]

Note that the band of CO linearly adsorbed on $Pd–In/Al_2O_3$ (2073 cm^{-1}) is shifted toward lower frequency by 15–20 cm^{-1}, as compared to the band of linear CO adsorbed on monometallic Pd/Al_2O_3 (2090 cm^{-1}). This shift can be explained by two effects. First, it points to the pronounced back-donation of electron density from the Pd atom to the anti-bonding π-orbital of the adsorbed CO molecule and a concomitant weakening of the C–O bond[19] indicating the modification of the Pd electronic states by covalent bonding in Pd–In. A similar effect was reported previously for Pd–Ga intermetallic catalysts.[10] Second, this shift may stem from a reduced lateral interaction between linearly adsorbed CO molecules due to the isolation of Pd sites by In atoms.

It is informative to estimate the strength of CO adsorption on Pd–In and Pd catalysts. For evaluating this parameter, the dynamics of CO desorption was studied by monitoring variations in the adsorbed CO band intensities upon purging the catalysts in an Ar flow at 50 °C after CO adsorption. Figure 2 shows the relationship between the relative intensity of the adsorbed CO band and purging time.

For the $Pd–In/Al_2O_3$ catalyst, the band intensity of linearly adsorbed CO at 2073 cm^{-1} decreases rapidly, and the band completely disappears after ~40 min. The dynamics of the linear CO desorption from Pd/Al_2O_3 is similar to that observed in $Pd–In/Al_2O_3$ during the first 15–20 min. However, after decreasing the intensity of a linearly adsorbed CO band by ~70%, the rate of CO desorption becomes distinctly slower. This observation suggests that the residual part of CO species is much stronger bound to the Pd surface, which can be explained by the strong

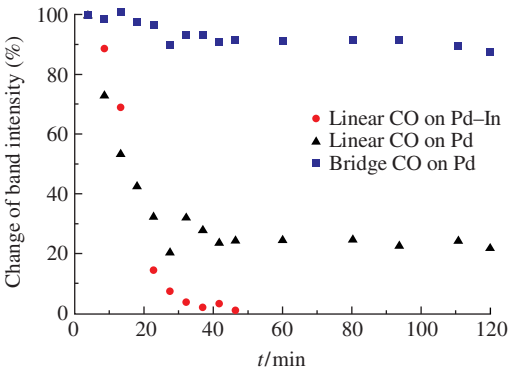

Figure 2 Dependence of the absorbed CO band intensities on purging time for $Pd–In/Al_2O_3$ and Pd/Al_2O_3 catalysts in an Ar flow.

binding of a CO molecule on corner and edge atoms with a high degree of coordination unsaturation. The bridge-bonded CO molecules in Pd/Al_2O_3 show considerably higher stability compared with that of the linearly adsorbed CO,[20] as indicated by the slow decrease in their band intensity.

Note that, unlike monometallic Pd/Al_2O_3, the bimetallic $Pd–In/Al_2O_3$ catalyst does not demonstrate a similar strong binding of the residual part of linearly adsorbed CO. Tentatively, the absence of strongly bound CO molecules indicates that Pd atoms on the surface of Pd–In nanoparticles are located mostly on terraces rather than corner or edge sites.

In general, a comparison between the dynamics of CO desorption from Pd/Al_2O_3 and $Pd–In/Al_2O_3$ demonstrates that the strength of CO adsorption on Pd–In is significantly reduced, as compared to the monometallic sample. This observation is consistent with data on the weakening of CO adsorption on PdGa due to a strong electronic perturbation of the Pd electronic state because of partial covalent Pd–Ga bonding.[10,12]

The stability of the Pd–In intermetallic surface and the single-atom structure of Pd active sites against oxidation at room temperature is essential for practical applications. For example, the surface structure of bimetallic Pd–Ga systems undergoes fast oxidation to metallic Pd and a mixture of palladium and gallium oxides in air under ambient conditions.[21] To estimate the stability of the PdIn surface structure, the freshly reduced $Pd–In/Al_2O_3$ catalyst was subjected to a series of consecutive oxidations by artificial air (20 vol% O_2/N_2) at 25 °C for 3, 7 and 10 min (Figure 3). After each oxidative treatment, the spectrum of adsorbed CO was measured to monitor changes in the surface structure.

We found that a short-time exposure (3 min) of the reduced $Pd–In/Al_2O_3$ to air resulted in a shift of a band at 2073 cm^{-1} to a higher frequency (2078 cm^{-1}) with the simultaneous appearance of a broad band (1965 cm^{-1}) corresponding to bridged CO species on metallic palladium. This clearly indicates the appearance of multiatomic Pd_n sites and suggests a partial destruction of the single-atom structure. The consecutive oxidative treatments for 7 and 10 min (Figure 3, curves *3* and *4*) led to a further gradual shift of the linearly adsorbed CO band to 2092 cm^{-1} typical of CO adsorbed on monometallic Pd/Al_2O_3. The peak of bridge-bonded CO shifted to 1970 cm^{-1}. Thus, the oxidation of the Pd–In catalyst for 10–20 min under ambient conditions is sufficient for inducing the destruction of the surface single-atom structure, the formation of Pd multiatomic centers, and a change in the electronic state of Pd.

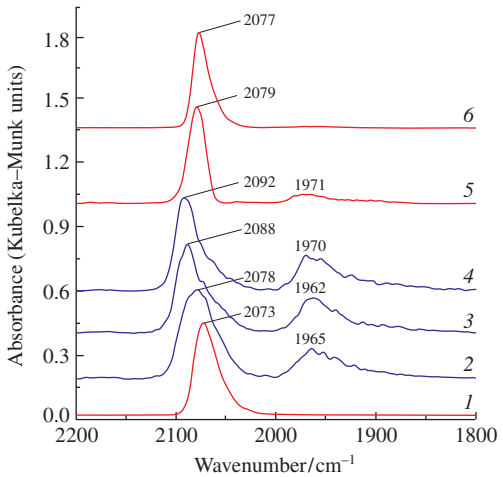

Figure 3 FTIR-CO spectra of $Pd–In/Al_2O_3$ after (*1*) reduction in H_2/Ar at 350 °C (1 h), after oxidation in air at 25 °C for (*2*) 3, (*3*) 7 and (*4*) 10 min, (*5*) after re-reduction in H_2/Ar at 150 °C (1 h), and (*6*) after re-reduction in H_2/Ar at 250 °C (1 h).

Presumably, the observed changes in the surface structure of Pd–In/Al_2O_3 resulted from the oxidation of In, partial destruction of the PdIn intermetallic surface, and the formation of a Pd-rich Pd–In intermetallic phase and In oxide patches that decorated palladium. A similar effect of oxidative treatment on the structure of Pd–Ga catalyst was reported previously.[22,23]

It is important that the single-atom structure of Pd active sites can be easily recovered by mild reduction at 150 °C (Figure 3, curve *5*). Reduction at 250 °C leads to the complete disappearance of the bridge-bonded CO band (Figure 3, curve *6*). This observation suggests that oxidation affects only a near-surface region, and it does not result in the significant segregation of Pd and In components. We can hypothesize that Pd sites, which remain metallic, activate hydrogen upon mild reduction and the facilitate the reduction of oxidized In species. Reduced indium species are easily incorporated into a near-surface area of palladium particles with the recovery of the initial Pd–In structure.

This study was supported by the Russian Science Foundation (grant no. 16-13-10530).

References

1 V. P. Ananikov, K. I. Galkin, M. P. Egorov, A. M. Sakharov, S. G. Zlotin, E. A. Redina, V. I. Isaeva, L. M. Kustov, M. L. Gening and N. E. Nifantiev, *Mendeleev Commun.*, 2016, **26**, 365.
2 P. V. Markov, G. O. Bragina, A. V. Rassolov, G. N. Baeva, I. S. Mashkovsky, V. Yu. Murzin, Ya. V. Zubavichus and A. Yu. Stakheev, *Mendeleev Commun.*, 2016, **26**, 502.
3 P. V. Markov, G. O. Bragina, A. V. Rassolov, I. S. Mashkovsky, G. N. Baeva, O. P. Tkachenko, I. A. Yakushev, M. N. Vargaftik and A. Yu. Stakheev, *Mendeleev Commun.*, 2016, **26**, 494.
4 A. A. Shesterkina, O. A. Kirichenko, L. M. Kozlova, G. I. Kapustin, I. V. Mishin, A. A. Strelkova and L. M. Kustov, *Mendeleev Commun.*, 2016, **26**, 228.
5 L. Zhang, A. Wang, J. T. Miller, X. Liu, X. Yang, W. Wang, L. Li, Y. Huang, C.-Y. Mou and T. Zhang, *ACS Catal.*, 2014, **4**, 1546.
6 G. X. Pei, X. Y. Liu, A. Wang, A. F. Lee, M. A. Isaacs, L. Li, X. Pan, X. Yang, X. Wang, Z. Tai, K. Wilson and T. Zhang, *ACS Catal.*, 2015, **5**, 3717.
7 A. V. Rassolov, P. V. Markov, G. O. Bragina, G. N. Baeva, D. S. Krivoruchenko, I. S. Mashkovskii, I. A. Yakushev, M. N. Vargaftik and A. Yu. Stakheev, *Kinet. Catal.*, 2016, **57**, 859 (*Kinet. Katal.*, 2016, **57**, 865).
8 S. Furukawa and T. Komatsu, *ACS Catal.*, 2017, **7**, 735.
9 S. Zafeiratos, S. Piccinin and D. Teschner, *Catal. Sci. Technol.*, 2012, **2**, 1787.
10 M. Armbrüster, M. Behrens, F. Cinquini, K. Föttinger, Yu. Grin, A. Haghofer, B. Klötzer, A. Knop-Gericke, H. Lorenz, A. Ota, S. Penner, J. Prinz, C. Rameshan, Z. Révay, D. Rosenthal, G. Rupprechter, Ph. Sautet, R. Schlögl, L. Shao, L. Szentmiklósi, D. Teschner, D. Torres, R. Wagner, R. Widmer and G. Wowsnick, *ChemCatChem*, 2012, **4**, 1048.
11 M. Neumann, D. Teschner, A. Knop-Gericke, W. Reschetilowski and M. Armbrüster, *J. Catal.*, 2016, **340**, 49.
12 M. Wencka, M. Hahne, A. Kocjan, S. Vrtnik, P. Koželj, D. Korže, Z. Jagličić, M. Sorić, P. Popčević, J. Ivkov, A. Smontara, P. Gille, S. Jurga, P. Tomeš, S. Paschen, A. Ormeci, M. Armbrüster, Yu. Grin and J. Dolinšek, *Intermetallics*, 2014, **55**, 56.
13 P. V. Markov, G. O. Bragina, G. N. Baeva, I. S. Mashkovskii, A. V. Rassolov, I. A. Yakushev, M. N. Vargaftik and A. Yu. Stakheev, *Kinet. Catal.*, 2016, **57**, 625 (*Kinet. Katal.*, 2016, **57**, 629).
14 P. V. Markov, G. O. Bragina, G. N. Baeva, O. P. Tkachenko, I. S. Mashkovskii, I. A. Yakushev, M. N. Vargaftik and A. Yu. Stakheev, *Kinet. Catal.*, 2016, **57**, 617 (*Kinet. Katal.*, 2016, **57**, 621).
15 X. P. Xu and D. W. Goodman, *J. Phys. Chem.*, 1993, **97**, 7711.
16 I. V. Yudanov, R. Sahnoun, K. M. Neyman, N. Rösch, J. Hoffmann, S. Schauermann, V. Johánek, H. Unterhalt, G. Rupprechter, J. Libuda and H.-J. Freund, *J. Phys. Chem. B*, 2003, **107**, 255.
17 H. L. Abbott, A. Aumer, Y. Lei, C. Asokan, R. J. Meyer, M. Sterrer, S. Shaikhutdinov and H.-J. Freund, *J. Phys. Chem. C*, 2010, **114**, 17099.
18 K. Kovnir, M. Armbrüster, D. Teschner, T. V. Venkov, F. C. Jentoft, A. Knop-Gericke, Yu. Grin and R. Schlögl, *Sci. Technol. Adv. Mater.*, 2007, **8**, 420.
19 K. Föttinger, J. A. van Bokhoven, M. Nachtegaal and G. Rupprechter, *J. Phys. Chem. Lett.*, 2011, **2**, 428.
20 H. Unterhalt, G. Rupprechter and H.-J. Freund, *J. Phys. Chem. B*, 2002, **106**, 356.
21 G. Wowsnick, D. Teschner, I. Kasatkin, F. Girgsdies, M. Armbrüster, A. Zhang, Yu. Grin, R. Schlögl and M. Behrens, *J. Catal.*, 2014, **309**, 209.
22 A. Haghofer, K. Föttinger, M. Nachtegaal, M. Armbrüster and G. Rupprechter, *J. Phys. Chem. C*, 2012, **116**, 21816.
23 R. Leary, F. de la Peña, J. S. Barnard, Y. Luo, M. Armbrüster, J. M. Thomas and P. A. Midgley, *ChemCatChem*, 2013, **5**, 2599.

Received: 25th April 2017; Com. 17/5235